Unconventional thin-film thermoelectric converters : structure, simulation, and comparative study

Maciej Haras, Valeria Lacatena, Stéphane Monfray, J.F. Robillard, Thomas Skotnicki, Emmanuel Dubois

Journal of ELECTRONIC MATERIALS, Vol. 43, No. 6, 2014
DOI: 10.1007/s11664-014-2982-z

Unconventional Thin-Film Thermoelectric Converters: Structure, Simulation, and Comparative Study

MACIEJ HARAS,[1,2,3] VALERIA LACATENA,[1,2] STÉPHANE MONFRAY,[2] JEAN-FRANÇOIS ROBILLARD,[1] THOMAS SKOTNICKI,[2] and EMMANUEL DUBOIS[1,4]

1.—IEMN UMR CNRS 8520, Institut d'Electronique, de Microélectronique et de Nanotechnologie, Avenue Poincaré, 59652 Villeneuve d'Ascq, France. 2.—STMicroelectronics 850, Rue Jean Monnet, 38926 Crolles, France. 3.—e-mail: Maciej.Haras@isen.iemn.univ-lille1.fr. 4.—e-mail: emmanuel.dubois@isen.iemn.univ-lille1.fr

Bi_2Te_3 or Sb_2Te_3 are the materials most widely used in thermoelectric generators (TEG) operating near room temperature. These materials are, however, environmentally harmful, expensive, and incompatible with complementary metal-oxide semiconductor (CMOS) technology, in contrast to silicon (Si), germanium (Ge), or silicon–germanium (SiGe). Although the thermopower (S) and electrical conductivity (σ) of Si and Ge are high, use in thermoelectricity is severely hindered by their high thermal conductivity (κ). By altering the phonon band structure of this Si films by use of an artificial phononic pattern, spectacular reduction of κ by two orders of magnitude has been demonstrated. To take full advantage of phonon band modification and scattering in thin films, converter structure based on thin-film membranes is proposed for κ reduction. To consolidate the position of Si-based materials, coupled charge and heat-transport simulations have been conducted to demonstrate the potential of the materials for thermoelectric conversion compared with such widespread materials as Bi_2Te_3. The effect of contact resistance on generator performance has been carefully taken into consideration to reflect integration constraints at the TEG level. For a temperature difference $\Delta T = 30$ K, the maximum electrical power density reaches approximately 6 W/cm^2 for Si and Ge, and approximately 3 W/cm^2 for $Si_{0.7}Ge_{0.3}$, values which are similar to those for Bi_2Te_3. Finally, it is emphasized that the proposed approach is compatible with conventional Si technology and naturally provides augmented mechanical flexibility that substantially widens the field of application of thermal harvesting.

Key words: Thermoelectric conversion, thermal conductivity reduction, CMOS compatible materials, harvested power density, thin-film, performance simulation

INTRODUCTION

Current thermoelectrics suffer from a lack of materials with sufficiently high conversion efficiency. Moreover, environmentally harmful, complex, and expensive materials and materials incompatible with complementary metal-oxide semiconductor (CMOS) technology are commonly used,[1,2] making fabrication costs relatively high. For all these reasons, applications of thermoelectric generators (TEG) are mainly limited to niche and sophisticated fields, e.g. automotive power generators,[3] spaceship generators,[4] industrial sensor feeders,[5] temperature measurements,[6] or advanced medical care.[7,8]

Thermoelectric conversion requires materials with low thermal conductivity (κ), high electrical conductivity (σ), and thermopower (S) as large as possible. On the basis of these criteria, the performance of thermoelectric materials is com-

(Received May 31, 2013; accepted January 2, 2014; published online January 22, 2014)

monly evaluated on the basis of the dimensionless figure-of-merit (zT):[9]

$$zT = \frac{S^2 \cdot \sigma}{\kappa} \cdot T = \frac{S^2 \cdot \sigma}{\kappa_e + \kappa_p} \cdot T, \quad (1)$$

$$\kappa_e(T) = L \cdot \sigma \cdot T, \quad (1a)$$

$$\kappa_p = v_s \cdot C_h \cdot \lambda/3, \quad (1b)$$

where κ can be separated into two contributions associated with heat transport by electrons and holes (κ_e) and by phonons (κ_p), T is the absolute temperature, L is the Lorenz factor, v_s is the velocity of sound, C_h the specific heat, and λ is the mean free path of phonons.

Figure 1a depicts, non-exhaustively, the state-of-the-art of conventional thermoelectric materials.

It is apparent that the operating temperature range of the converter is crucially important in choosing a thermoelectric material. To maximize conversion efficiency the material with the highest zT in the region of the targeted operating temperature should be used. The relationship between zT and the efficiency of an ideal converter is:[11]

$$\eta = \frac{T_{HOT} - T_{COLD}}{T_{HOT}} \cdot \frac{\sqrt{1+zT} - 1}{\sqrt{1+zT} + \frac{T_{COLD}}{T_{HOT}}}. \quad (2)$$

Conversion efficiency as a function of temperature is shown in Fig. 1b for different zT values. Red markers are representative of the highest efficiency for a given material. According to Tritt et al.,[12] the quest for both n-type and p-type materials with:

1 reduced thermal conduction losses;
2 zT in the range 2–3; and
3 small fabrication costs

still constitutes a "Holy Grail" for more widespread use of thermoelectrics. S and σ of semiconductors can be easily controlled by adjusting the doping level. However, the thermal conductivity due to charged carriers (κ_e) is also closely related to electrical conductivity by the Wiedemann–Franz law formalized by Eq. 1b. This observation therefore reveals inherent material optimization conflicts insofar as increasing the electrical conductivity negatively affects both S and κ. Nevertheless, phonon heat transport (κ_p) dominates in most bulk semiconductors and is responsible for over 95% of thermal conduction. To reduce κ without changing electrical properties substantially, κ_p must therefore be reduced without altering κ_e. Although silicon (Si) and germanium (Ge) have high S and σ, their use in thermoelectricity is severely hindered by their high κ, which dramatically reduces zT. Interestingly, bulk SiGe has a significantly lower (8 W/m/K)[13] thermal conductivity than bulk Si (148 W/m/K)[14] and bulk Ge (60 W/m/K)[15] over a wide range of Ge content (between 20% and 80%), as shown in Fig. 2a.

It has been demonstrated that if the phonon band structure of Si thin films is altered by use of an artificial phononic pattern, κ is spectacularly reduced by two orders of magnitude;[16–18] this is depicted in Fig. 2b.

In this paper, particular emphasis is placed on use of Si, Ge, or SiGe combined with thin-film phononic engineering to reduce the phononic thermal conductivity κ_p (Eq. 1b) below that of the electronic counterpart κ_e. In this situation, the properties of Si, Ge, and SiGe phononic membranes approach the ideal property of a *phonon glass/electron crystal*[19] for which ZT converges toward S^2/L, the asymptotic limit that ensues directly from Eq. 1 when κ_p is small compared with κ_e.

STRUCTURE

The possibility of introducing in-plane membranes to TEG was discussed more than a decade ago[20] and was further developed for co-evaporated V–VI compounds.[21,22] This work was conducted to investigate how the performance of clean, safe, and

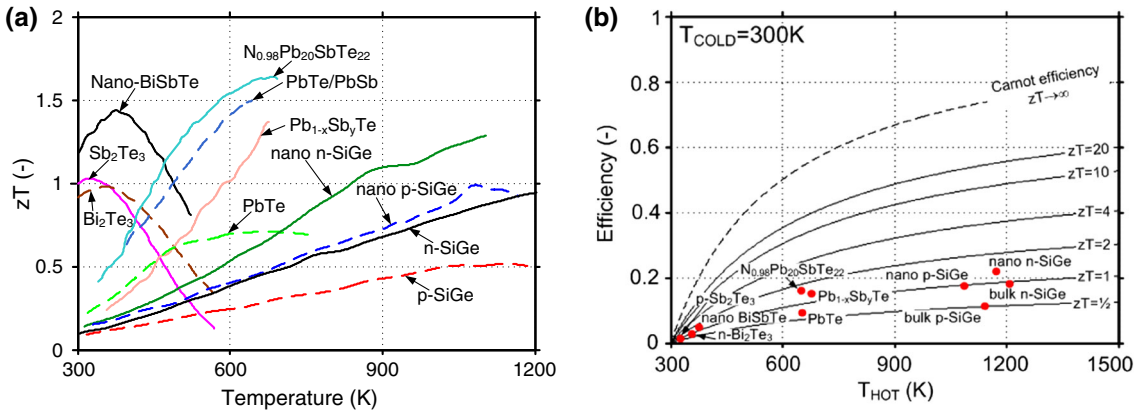

Fig. 1. (a) Dimensionless figure-of-merit for different materials as a function of temperature (after Minnich et al.[10] and Snyder et al.[1]). (b) Temperature dependence of conversion efficiency for different zT values. Red dots show the highest efficiency for a selection of materials.

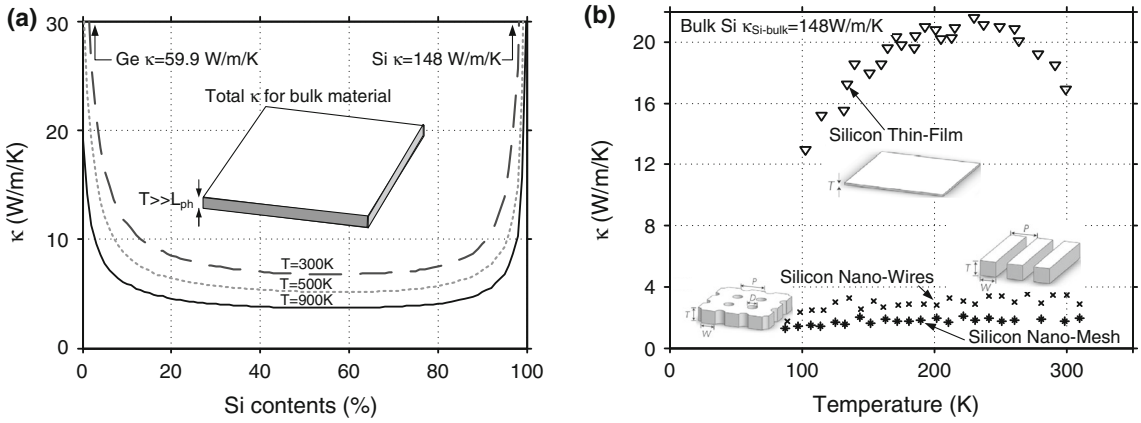

Fig. 2. CMOS-compatible materials and their thermal conductivity. κ (a) Si_xGe_{1-x} thermal conductivity as a function of Si content for different temperatures (based on Ref. 13), (b) reduction of the thermal conductivity of silicon (from Ref. 16).

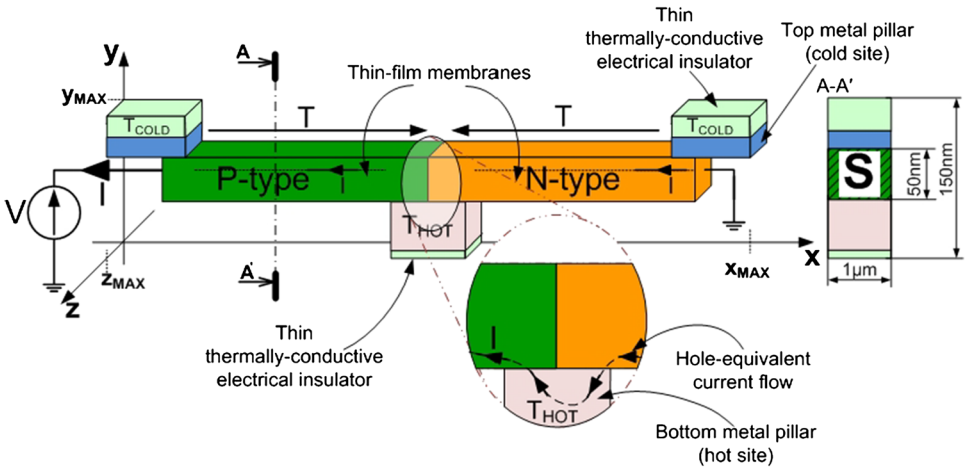

Fig. 3. Structure of a membrane Seebeck generator with use of CMOS-compatible thin-film membranes. x_{MAX} = 10 μm (single membrane length 5 μm), y_{MAX} = 150 nm (50 nm membrane thickness), z_{MAX} = 1 μm.

abundant materials, for example Si, SiGe, and Ge, used in mainstream CMOS technology, could be elevated to a level similar to that of thermoelectric materials containing lead, antimony, and other harmful substances. The structure of a membrane-based Seebeck generator is presented in Fig. 3. One prerequisite for benefitting from enhanced phonon scattering is use of a thin-film membrane. A second condition for further reduction of κ_p is to superimpose a phononic crystal pattern on this membrane to obtain the above-mentioned κ_p reduction.

Following this strategy, it is worth noting that the horizontal membrane structure also redirects heat flow from the vertical to the lateral direction. From a practical perspective, this structure also leads to converter geometry with extremely low thickness. This remarkable feature renders this type of converter readily able to accommodate flexure. Mechanical flexibility can be a crucial property if generators are installed on, e.g., hot pipes, exhaust systems, or textiles etc.

SIMULATION MODEL

To investigate performance of the proposed converter structure, simulations based on coupled resolution of carriers and heat-transport equations were performed. In our simulation current densities follow the non-isothermal drift–diffusion model:[23]

$$\begin{cases} \vec{j}_n(T) = -\sigma_n(T) \cdot \left[\vec{\nabla}\varphi_{Fn}(T) - S_n(T) \cdot \vec{\nabla}T\right] \\ \vec{j}_p(T) = -\sigma_p(T) \cdot \left[\vec{\nabla}\varphi_{Fp}(T) - S_p(T) \cdot \vec{\nabla}T\right] \end{cases}, \quad (3)$$

where

$$\begin{cases} \varphi_{Fn}(T) = \phi - \dfrac{k \cdot T}{q} \ln\left[\dfrac{n(T)}{n_i(T)}\right] \\ \varphi_{Fp}(T) = \phi + \dfrac{k \cdot T}{q} \ln\left[\dfrac{p(T)}{n_i(T)}\right] \end{cases}, \quad \begin{cases} \sigma_n(T) = q \cdot \mu_n(T) \cdot n(T) \\ \sigma_p(T) = q \cdot \mu_p(T) \cdot p(T) \end{cases} \text{ and } \quad \begin{cases} S_n(T) = -\dfrac{k}{q} \cdot \left[\dfrac{3}{2} + \ln\left(\dfrac{N_c(T)}{n(T)}\right)\right] \\ S_p(T) = \dfrac{k}{q} \cdot \left[\dfrac{3}{2} + \ln\left(\dfrac{N_v(T)}{p(T)}\right)\right] \end{cases} \quad (4)$$

The constitutive current relationships given in Eq. 3 enable such temperature-dependent properties as carrier mobility (μ_n, μ_p), electrical conductivity (σ_n, σ_p), carrier concentrations (n, p), or quasi-Fermi levels (ϕ_{Fn}, ϕ_{Fp}) to be taken into account. Here, the temperature considered is the local lattice temperature (T).

RESULTS

Effect of Doping Level on *I–V* Characteristics in the Generator Zone

According to Fig. 3, a metallic ohmic contact is located at every PN junction to act as an electrical short. Figures 4a and b show the *I–V* characteristics of Si membranes with high (10^{19} cm^{-3}) and low (10^{15} cm^{-3}) doping levels, respectively. Only the fourth quadrant of the *I–V* chart is represented, because it corresponds to the generator mode. Although thermopower is higher at low doping levels, Fig. 4b reveals a dramatic current limitation for lightly doped membranes.

Harvested Power Density for Si, Ge, and SiGe

To compare the harvesting capabilities of Si, Ge, and SiGe with those of widely used materials, for example Bi_2Te_3 alloys, the power density was calculated as a function of the voltage generated, assuming that the temperature gradient across the generator is constant. By following this method, it is, therefore, possible to compare the aforementioned materials on the basis of Seebeck and electrical conductivity performance, irrespective of their thermal conductivity. Naturally, one prerequisite that legitimates this method is to consider that phononic engineering of thin membranes can be independently used to cut thermal conductivity for Si and Ge. Beyond the electrical conductivity of the intrinsic thermoelectric material, the metal–semiconductor contact resistance must be taken into consideration to properly reflect electrical performance.[24] In the calculation of the power density, we have assumed a specific contact resistivity of 5×10^{-7} Ω cm^2 for Si and SiGe. Given the maturity of Ni and Pt-based silicide and germano-silicide technology, this figure realistically corresponds to a worst-case analysis.[25,26] Although contact resistance to *n*-type Ge has long remained a problem, because of strong Fermi level pinning close to the valence band, recent work has shown that this effect is spectacularly alleviated by inserting an ultra-thin dielectric layer between the metal and the semiconductor.[27] For this reason, the same value of specific contact resistivity, i.e. 5×10^{-7} Ω cm^2, can be reasonably assumed for Ge. The situation differs for Bi_2Te_3, for which common values of specific contact resistivity are between 1.45×10^{-7} Ω cm^2 [28] and 10^{-5} Ω cm^2, the latter value being identified in Ref. 29 as a representative figure when standard processing techniques are used for contact realization. In our analysis, simulations associated with Bi_2Te_3 have been performed for the two extremes of this range, and Seebeck and electrical conductivity were taken from the modeling work described in Ref. 30. This model is temperature-dependent and follows with good precision data measured for Bi_2Te_3 at the same temperature difference.[31–35] Variation of the harvested power density as a

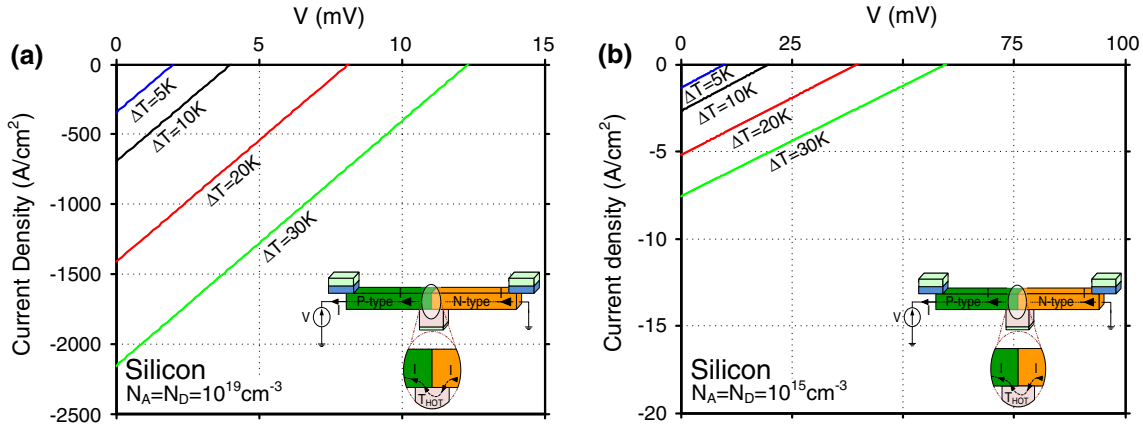

Fig. 4. Harvested current density as a function of voltage for different temperatures differences (s = 50 nm × 1 μm) in the generator zone (fourth quadrant) for (a) heavily doped silicon thin-film membranes and (b) lightly doped silicon thin-film membranes.

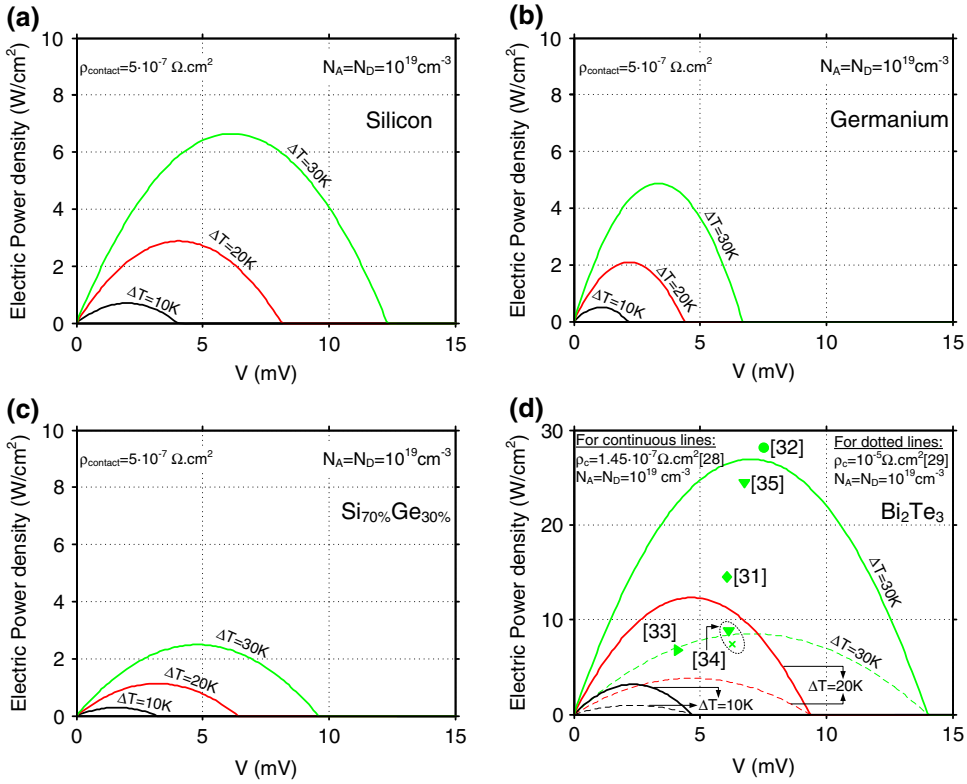

Fig. 5. Harvested electric power density as a function of generator output voltage for membrane Seebeck generator, (a) membranes made from silicon, (b) membranes made from germanium, (c) membranes made from $Si_{70\%}Ge_{30\%}$, and (d) membranes made from bismuth telluride with thermoelectric properties in accordance with Ref. 30 Isolated markers correspond to maximum harvested power density for ΔT = 30 K calculated from the measured values of σ_n, σ_p, S_n, S_p quoted in each of the associated literature references.

function of output voltage for different temperatures is presented in Fig. 5 .

Figures 5a–c depict the harvested power density as a function of output voltage for the proposed generator topology based on CMOS core materials. For comparison purposes, Fig. 5d also depicts the power density associated with Bi_2Te_3 for the same generator geometry. Depending on contact quality, it can be observed that harvested power density for Si, SiGe, and Ge is slightly lower than that for Bi_2Te_3, the performance of which depends critically on the specific contact resistivity achievable. This conclusion is consolidated in Fig. 6, in which the maximum harvested power densities for the materials are compared. This figure was obtained under load-matching conditions[36] for which the load and internal generator resistances were equal.

Although Si, Ge, and SiGe harvest a lower power density than Bi_2Te_3 for a same temperature gradient, it is worth emphasizing that they are compatible with conventional CMOS technology, making integration of TEGs possible. It is note worthy that SiGe harvests less power than Si or Ge for the same ΔT. This can be readily explained by the lower electrical conductivity of SiGe compared to Si and Ge at identical doping level. However, because of a lower κ (Fig. 2a), it is expected that SiGe will convert heat with higher efficiency than Si or Ge.

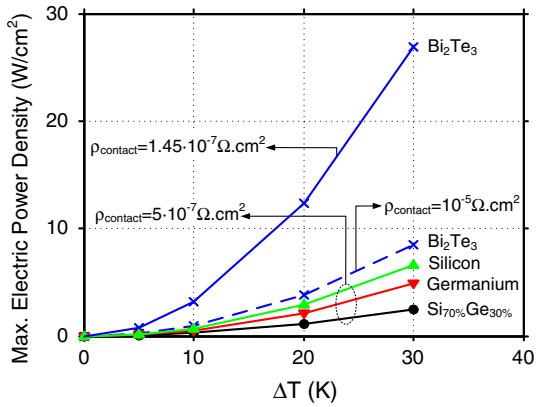

Fig. 6. Maximum electric power density as a function of temperature difference for membrane Seebeck generators with membranes made from the materials investigated taking into account the parasitic effect of contact resistance.

CONCLUSIONS

Si, Ge, and SiGe have interesting thermoelectric properties and could be turned into good thermoelectric materials by a significant reduction of their thermal conductivity. For this purpose, recent advances in Si membranes fabrication and phononic engineering are promising technology. Reduction of the thermal conductivity of Si, Ge, and SiGe by two

order of magnitude can be achieved, making those materials very attractive for future TEG. In this paper, we have proposed the innovative topology of a Seebeck membrane generator based on thin-film single-crystal CMOS-compatible materials that could exploit such effects. Our results show that the electric power density of Si, Ge, and SiGe and Bi_2Te_3 membrane-based TEGs are of the same order of magnitude. Moreover use of Si, Ge, and SiGe enables compatibility with the production technology used for conventional semiconductor devices.

REFERENCES

1. G.J. Snyder and E.S. Toberer, *Nat. Mater.* 7, 105 (2008).
2. T.M. Tritt, *Annu. Rev. Mater. Res.* 41, 433 (2011).
3. J. Yang and T. Caillat, *MRS Bull.* 31, 224 (2006).
4. D.M. Rowe, *Appl. Energy* 40, 241 (1991).
5. P. Nenninger and U. Marco, *ABB Rev.* 1, 47 (2011).
6. J. P. Carmo, L. M. Goncalves, and J. H. Correia, in *Scanning Probe Microscopy in Nanoscience and Nanotechnology*, vol. 2.2, ed. by B. Bhushan (Springer, Heidelberg, 2010), pp. 791–811.
7. V. Leonov, P. Fiorini, T. Torfs, R. J. M. Vullers, and C. Van Hoof, in *15th International Workshop on Thermal Investigations of ICs and Systems (Therminic)* (2009), pp. 95–100.
8. L. Francioso, C. De Pascali, I. Farella, C. Martucci, P. Cretì, P. Siciliano, and A. Perrone, *J. Power Sources* 196, 3239 (2011).
9. D.M. Rowe, *Proc. IEE* 125, 1113 (1978).
10. J. Minnich, M.S. Dresselhaus, Z.F. Ren, and G. Chen, *Energy Environ. Sci.* 2, 466 (2009).
11. G. Min and D.M. Rowe, *IEEE Trans. Energy Convers.* 22, 528 (2007).
12. T.M. Tritt, H. Böttner, and L. Chen, *MRS Bull.* 33, 366 (2008).
13. B. Abeles, *Phys. Rev.* 131, 1906 (1963).
14. W. Fulkerson, J.P. Moore, R.K. Williams, R.S. Graves, and D.L. McElroy, *Phys. Rev.* 167, 765 (1968).
15. C.J. Glassbrenner and G.A. Slack, *Phys. Rev.* 134, A1058 (1964).
16. J.-K. Yu, S. Mitrovic, D. Tham, J. Varghese, and J.R. Heath, *Nat. Nano* 5, 718 (2010).
17. P.E. Hopkins, C.M. Reinke, M.F. Su, R.H. Olsson, E.A. Shaner, Z.C. Leseman, J.R. Serrano, L.M. Phinney, and I. El-Kady, *Nano Lett.* 11, 107 (2011).
18. D. Narducci, G. Cerofolini, M. Ferri, F. Suriano, F. Mancarella, L. Belsito, S. Solmi, and A. Roncaglia, *J. Mater. Sci.* 48, 2779 (2012).
19. G.A. Slack, *CRC Handbook of Thermoelectrics* (Boca Raton: CRC Press, 1995).
20. J. Nurnus, H. Bottner, and A. Lambrecht, in *Twenty-Second International Conference on Thermoelectrics ICT* (2003), pp. 655–660.
21. L.M. Goncalves, J.G. Rocha, C. Couto, P. Alpuim, G. Min, D.M. Rowe, and J.H. Correia, *J. Micromech. Microeng.* 17, S168 (2007).
22. J. Kurosaki, A. Yamamoto, S. Tanaka, J. Cannon, K. Miyazaki, and H. Tsukamoto, *J. Electron. Mater.* 38, 1326 (2009).
23. G. K. Wachutka, in *IEEE Transactions on Computer-Aided Design of Integrated Circuits and Systems*, vol. 9 (IEEE, New York, 1990), p. 1141.
24. G. Min and D.M. Rowe, *Solid-State Electron.* 43, 923 (1999).
25. N. Stavitski, M.J.H. van Dal, A. Lauwers, C. Vrancken, A.Y. Kovalgin, and R.A.M. Wolters, *IEEE Electron Device Lett.* 29, 378 (2008).
26. Z. Zhang, S.O. Koswatta, S.W. Bedell, A. Baraskar, M. Guillorn, S.U. Engelmann, Y. Zhu, J. Gonsalves, A. Pyzyna, M. Hopstaken, C. Witt, L. Yang, F. Liu, J. Newbury, W. Song, C. Cabral, M. Lofaro, A.S. Ozcan, M. Raymond, C. Lavoie, J.W. Sleight, K.P. Rodbell, and P.M. Solomon, *IEEE Electron Device Lett.* 34, 723 (2013).
27. J.-Y.J. Lin, A.M. Roy, and K.C. Saraswat, *IEEE Electron Device Lett.* 33, 1541 (2012).
28. R. Venkatasubramanian, E. Siivola, T. Colpitts, and B. O'Quinn, *Nature* 413, 597 (2001).
29. L. W. da Silva, and M. Kaviany, in *ASME International Mechanical Engineering Congress and Exposition*, New Orleans, USA (ASME, New York, 2002), pp. 1–15.
30. X. Luo, M.B. Sullivan, and S.Y. Quek, *Phys. Rev. B* 86, 184111 (2012).
31. M. Mizoshiri, M. Mikami, and K. Ozaki, Jpn. J. App. Phys. 52, 06GL07 (2013).
32. H.J. Goldsmid, A.R. Sheard, and D.A. Wright, *Br. J. Appl. Phys.* 9, 365 (1958).
33. C.-H. Kuo, C.-S. Hwang, M.-S. Jeng, W.-S. Su, Y.-W. Chou, and J.-R. Ku, *J. Alloys Compd.* 496, 687 (2010).
34. L. M. Goncalves, in *Thermoelectrics and Its Energy Harvesting*, ed. by D. M. Rowe (CRC Press, Boca Raton, 2012), pp. 407–426.
35. H. Scherrer and S. Scherrer, *CRC Handbook of Thermoelectrics* (Boca Raton: CRC Press, 1995).
36. M. Strasser, R. Aigner, C. Lauterbach, T.F. Sturm, M. Franosch, and G.K.M. Wachutka, *Sensors Actuators Phys.* 114, 362 (2004).